15-Hydroxyeicosatetraenoic Acid and GPR39 Together Orchestrate Coronary Autoregulation: A Comprehensive Metabolomic Analysis

D. Elizabeth Le, M.D.[1,2]
Masaki Kajimoto, M.D., Ph.D.[1]
Yan Zhao, M.D.[1]
Carmen Methner, Ph.D.[1]
Zhiping Cao, Ph.D.[1]
Agostino Cianciulli, Ph.D.[4]
Teresa Semeraro, Ph.D.[4]
Iuni Margaret Laura Trist, Ph.D.[4]
Jessica Franchi, M.Sc.[4]
Chiara Marcheselli, PhD[4]
Alberto Parazzoli, PhD[4]
Fabrizio Micheli, Ph.D.[4]
Sanjiv Kaul, M.D.[1,3]
(Orchid ID 0000-0003-0124-3920)

From the [1]Knight Cardiovascular Institute, [2]Veterans Administration Portland Health Care System, Oregon Health & Science University, [3]Vasocardea, Inc. Portland, Oregon, USA, and [4]Aptuit (Evotec), Verona, Italy

Supported, in part, by grants from the Garthe and Grace L. Brown Fund and the John E. and Robin Jaqua Fund at the Oregon Community Foundation, and by the Ernest C. Swigert endowment at the Oregon Health & Science University

Running title: 15-HETE and GPR39 in coronary autoregulation

Word count: 8331 (excluding Tables)

Address correspondence to:

Sanjiv Kaul, M.D.
Knight Cardiovascular Institute
Oregon Health & Science University
UHN62
3181 SW Sam Jackson Park Rd.
Portland, OR 97239

E: kauls@ohsu.edu
T: 503-494-3889
F: 503-494-8550

Abstract

Background: Coronary autoregulation is the ability of the normal heart to maintain constant coronary blood flow (CBF) over a wide range of coronary driving pressures (CDP). Despite being vital for survival, the mechanism of coronary autoregulation is unknown. We hypothesized that GPR39, present in vascular smooth muscle cells, together with its endogenous agonist 15-hydroxyeicosatetraenoic acid (15-HETE) orchestrate coronary autoregulation.

Methods: We created coronary stenoses of varying degrees in open-chest, anesthetized dogs where we measured CBF and CDP. In a subset of animals, coronary venous blood was sampled for eicosanoid, adenosine, endothelin-1, polyunsaturated fatty acids, and prostaglandins levels. Stenoses were recreated during intravenous administration of VC108, a specific GPR39 antagonist and systemic, pulmonary, and coronary hemodynamics measured.

Results: GPR39 was identified in coronary arterioles by immunohistochemistry and in heart tissue by western blot. In-vivo, 15-HETE correlated linearly with CDP over the autoregulatory range (r^2=0.47, p=0.0024). Apart from 6-keto $PGF1_{\alpha}$ no other metabolite had any relation with CDP. Prior to administration of VC108, CBF did not change within the autoregulatory range. VC108 had no effect of systemic and pulmonary hemodynamics but increased CBF (p=0.02 versus vehicle) by decreasing coronary microvascular resistance (p=0.01 versus vehicle), indicating that GPR39 participates in control of normal coronary vascular tone. With VC108, coronary autoregulation was abolished and CBF became CDP dependent (r^2=0.96, p=0.004).

Conclusion: GPR39 and its endogenous agonist 15-HETE together orchestrate coronary autoregulation when CDP is reduced. These novel findings provide a mechanism for coronary autoregulation and could direct pharmacological treatment of various coronary syndromes in humans.

Key words: Coronary autoregulation; 15-HETE; GPR39

Non-standard Abbreviations and Acronyms

14,15-EET	14,15-epoxyeicosatrienoic acid
15-HETE	15-hydroxyeicosatetraenoic acid
CBF	coronary blood flow
CDP	coronary driving pressure
COX-1	cyclooxygenase-1
DHET	Dihydroxyeicosatrienoic acid
DMSO	dimethyl sulfoxide
EDTA	Ethylenediaminetetraacetic acid
eNOS	endothelial NO synthetase
ERK	extracellular signal-regulated kinase
Gαq	G-protein αq
GPR39	G-protein coupled receptor
H_2O_2	hydrogen peroxide
LOX	lipoxygenase
MVR	microvascular resistance
NO	nitric oxide
PGD2	prostaglandin D2
PGE2	prostaglandin E2
PGF2α	prostaglandin F2α
PLA_2	phospholipase A2
RA	right atrial
TBXA2	thromboxane A2
VSMC	vascular smooth muscle cell

94

Coronary autoregulation refers to the ability of the normal heart to maintain constant coronary blood flow (CBF) over a wide range of coronary driving pressures (CDPs) provided cardiac work remains constant. Lowering CDP results in vasodilation of the resistance arterioles present within the heart while raising CDP cause vasoconstriction of these vessels, thus maintaining constant CBF.[1-4] Autoregulation is a teleologically protective mechanism that is meant to keep blood flow constant to vital organs despite wide alterations in systemic pressures and ensure a constant capillary hydrostatic pressure necessary for cell survival.[5] In large animals and humans, the CDP range where CBF remains constant is between approximately 45 to 120 mm Hg.[1-4]

Despite the relevance of coronary autoregulation to survival, its mechanism is unknown.[6] The eicosanoid 20-hydroxyeicosatetraenoic acid (20-HETE) has been implicated in cerebral autoregulation.[7] Eicosanoids form a wide variety of lipid-based signaling molecules present in various forms and concentrations in different tissues.[8] Although some eicosanoids are vasoactive, their role in coronary autoregulation has not been examined. Further, while single mediators like adenosine have been investigated as a putative mechanism of coronary autoregulation[9,10] a comprehensive metabolomic analysis of all possible vasoactive compounds that could influence resting coronary vascular tone and coronary autoregulation has not been performed.

We reported the presence of a G-protein coupled receptor (GPR39) in the vascular smooth muscle cells (VSMCs) of coronary arterioles in the mouse heart.[11] We showed that two eicosanoids are endogenous ligands for GPR39: 15-hydroxyeicosatetraenoic acid (15-HETE) is the agonist, and 14,15-epoxyeicosatrienoic acid (14,15-EET) is the antagonist. GPR39 stimulation by 15-HETE activates phospholipase C through the Gαq pathway that cleaves

membrane bound inositol phosphatidylinositol 4,5-bisphosphate (PIP2) into inositol 1,4,5-trisphosphate (IP3) and diacylglycerol (DAG). DAG remains in the cell membrane while IP3 binds to the IP3 receptors on the endoplasmic reticulum, releasing Ca^{++} into the cytosol, causing cell contraction.[11] Ca^{++} also acts as a second messenger causing extracellular signal-regulated kinase (ERK) phosphorylation leading to additional downstream effects.[11]

Both 15-HETE (vasoconstrictor) and 14,15-EET (vasodilator) act through GPR39 to maintain coronary vascular tone.[11] Consequently, we hypothesized that the levels of 15-HETE and 14,15-EET, acting on GPR39, will determine coronary vascular tone depending on the CDP. We postulated that the receptor and its ligands together orchestrate coronary autoregulation.

Methods

A canine model was selected for the autoregulation study because coronary physiology can be reliably studied in these animals and because most of the classical papers on coronary autoregulation were performed in this model. The data that support the findings of this study are available from the corresponding author upon reasonable request. Results are reported according to ARRIVE guidelines. The study protocols were approved by the Institutional Animal Care and Use Committee at the Oregon Health & Science University and conformed to the National Institutes of Health guidelines for animal research.

Animal Preparations

For the autoregulation study, 35 adult male mongrel dogs (30-35 kg) were studied. Females were excluded because of possible pregnancy and uncertainty of timing in the ovulation cycle. Dogs were sedated with intramuscular injection of hydromorphone (0.1-0. 2 mg□Kg^{-1}) and then induced with intravenous administration of ketamine (2-5 mg□Kg^{-1}) and midazolam (0.1-0.4 mg□Kg^{-1}). They were then intubated and ventilated (Integra SL with AV-S ventilator,

Avante Health Solutions, Louisville, KY, USA) with isoflurane gas (0.5-1.0%) and medical-grade room air. Constant-rate infusion anesthesia was maintained with intravenous administration of ketamine (0.3-0.5 mg□Kg^{-1} bolus followed by an infusion of 0.3-1.5 mg□$Kg^{-1}hr^{-1}$), fentanyl (0.001-0.003 mg bolus followed by an infusion of 0.05-0.07 µg□$Kg^{-1}min^{-1}$), and a very low dose lidocaine infusion (0.6-6.0 mg□$Kg^{-1}hr^{-1}$ IV). These infusion rates of the drugs were adjusted throughout the experiment to optimize anesthesia without affecting coronary reactivity. The mean coronary hyperemic response after a 20 s occlusion was 3-fold, which is normal in open-chest dogs indicating that anesthesia did not affect vasomotor tone.

Heart rate, blood pressure, O_2 saturation, end-tidal CO_2, and temperature were continuously monitored (Advisor® Vital Signs Monitor, Surgivet, Norwell, MA, USA). A 6F sheath was inserted in the right femoral artery for arterial pressure measurement. 7F catheters were inserted into the right femoral, right atrium (RA), and peripheral veins for administration of drugs and fluids and measurement of pressure. In a subset of animals, a 7F sheath was inserted for placement of a balloon-tipped catheter (Edwards Lifesciences, Santa Ana, CA, USA) for measurement of pulmonary artery (PA) pressures. In the same dogs a micromanometer-tipped catheter (Millar Instruments, Inc., Houston, TX, USA) was inserted into the left ventricular cavity to measure left ventricular $\Delta P/\Delta t$.

A left lateral thoracotomy was performed, and the heart was suspended in a pericardial cradle. The left anterior descending (LAD) coronary artery was dissected free from surrounding structures in its proximal and mid portions. An ultrasonic time-of-flight flow probe (Series SC, Transonics, Ithaca, NY, USA) was placed on the proximal segment of the artery and connected to a digital flow meter (Model T206, Transonics). A screw occluder was positioned around the mid-portion of the artery to create coronary stenoses of varying degrees. A 20-gauge

polyethylene catheter was inserted into the distal portion of the artery to measure pressure. A similar catheter was inserted in the anterior cardiac vein for obtaining blood samples. CDP was calculated as the difference between the distal LAD and RA pressures. Coronary microvascular resistance (MVR) was derived by the CDP/CBF ratio.

Hemodynamic Measurements

All catheters and flow meters were interfaced with a multi-channel recorder (PowerLab, AD Instruments, Inc., Colorado Springs, CO, USA). Phasic and mean CBF and systemic pressures were acquired digitally and displayed on-line on an iMac (Apple Inc., Cupertino, CA, USA). All data were analyzed off-line using LabChart 6.

Mass Spectroscopy

The details for mass spectroscopy measurements of lipids and adenosine have been published before.[12,13] For measurement of eicosanoids and prostaglandins blood was drawn in a stop solution containing 8 mg butylated hydroxytoluene and 80 mg triphenylphosphonium mixed with 80 mg indomethacin in 40 mL methanol solution. The samples were centrifuged, placed on ice and sent for analysis.

Measurements were made using MS/MS with a 5500 Q-TRAP hybrid/triple quadrupole linear ion trap mass spectrometer (Applied Biosystems, Waltham, MA, USA) with electrospray ionization (ESI) in negative mode. The mass spectrometer (MS/MS) was interfaced to a Shimadzu (Columbia, MD, USA) SIL-20AC XR auto-sampler followed by 2 LC-20AD XR LC pumps and analysis on an Applied Biosystems/SCIEX Q5500 instrument. The instrument was operated with the following settings: source voltage -4000 kV, GS1 70, GS2 70, CUR 45, TEM 750 and CAD gas MED. The gradient mobile phase was delivered at a flow rate of 0.5 mL/min, and consisted of two solvents, A: 0.05% acetic acid in water and B: acetonitrile. The LC column used was a Kinetex Phenyl-Hexyl 50x2.1 mm 2.6 µM. The initial concentration of solvent B

used was 20%, this was held for 0.5 minutes, increased to 60% B over 10.5 minutes, increased to 95% B over 1 min, held at 95% B for 1 min, and then returned to initial conditions over 0.1 min, followed by re-equilibration for 1.9 min for a total run time of 15 min. The column oven was set to 50°C, autosampler to 15°C with needle rinse before and after each injection. Data was acquired using Analyst 1.7.1 and analyzed with Multiquant 3.03.

For arachidonic acid and other polyunsatured fatty acids, analysis was performed using an Agilent 7890B GC (Santa Clara, CA, USA) with a 5977A MS detector with an autosampler and split/splitless injector operated in split mode. The column was an Agilent DB-FastFAME column (30 m, 0.25 mm id, 0.25 μm film thickness). Helium was the carrier gas at a flow rate of 1 mL/min. The injection port and auxiliary heater were maintained at 245°C. A 1 μL sample was injected in split mode (1:10) at an initial oven temperature of 150°C, held for 0.5 min and then increased at 15°C/min to 200°C, followed by 25°C/min to 240°C, held for 2 min and then returned to 50°C. The MS was operated at a source temperature of 230°C and a MS quad temperature of 150°C in positive electron impact mode. The GC-MS data were acquired using enhanced MassHunter software. Calibration curves for quantification were generated from peak area ratios for authentic standard:internal standard for calibrator samples.

For adenosine, blood was obtained in stop solution containing dipyridamole, sodium EDTA, erythro-hydroxy-nonyladenine, α,β-methylene-adenosine 5'-diphosphatenucleotidase, and heparin.[14] The sample was centrifuged, placed on ice, and sent for analysis. Plasma was analyzed using MS/MS with a 5500 Q-TRAP PLUS hybrid/triple quadrupole linear ion trap mass spectrometer (Applied Biosystems) with electrospray ionization (ESI) in positive mode. The tandem MS/MS was interfaced to a Shimadzu SIL-20AC XR auto-sampler followed by 2 LC-20AD XR LC pumps. The MS instrument was operated with the following settings: source

voltage 5500 kV, GS1 60, GS2 560, CUR 35, TEM 750, and CAD gas MED. Compounds were infused individually and MS/MS instrument parameters optimized for each MRM transition. Those used for quantification were *m/z*=268→136 for adenosine with a dwell time of 100 msec, DP= 75, EP=10, CXP=15 and CE=25 and *m/z*=273.2→136 with a dwell time of 100 msec, DP= 75, EP=10, CXP=15 and CE=25. Data was acquired using Analyst 1.7.3 and analyzed with Multiquant 3.03.

For VC108 measurements, a 12-point calibration curve and quality control samples were prepared in blood diluted 1:4.8 in 0.1N Hepes buffer in micronic tubes., 20 µL of which was transferred into micronic tubes containing 80µL 0.1N Hepes buffer. Calibration samples, quality control samples, and analysis samples were extracted by adding 400µL CH3CN containing IS (Rolipram) 20 ng/mL.

After vortex and centrifugation (3000 rpm/10 min), samples supernatants were transferred to a 96 well plate and diluted (450µL CH3CN/aq=37/63 + 50µL supernatant). Samples were injected using an Agilent 1290 Infinity II UPLC system (Santa Clara, CA, USA) and separated on a Acquity UPLC BEH C18 (30x2.1mm, 1.7µm, Milford, MA, USA) connected directly to the TurboIonSpray source of an AB Sciex 6500QTrap mass spectrometer (Framingham, MA, USA). Mobile Phase A was 0.1% (v/v) formic acid in water and Mobile Phase B was 0.1% (v/v) formic acid in acetonitrile. The flow rate was 1 mL/min and a generic gradient of 5% B to 95% B in 1.3min was applied.

ELISA for Endothelin-1

Plasma samples were analyzed for endothelin-1 using an ELISA kit (Catalog# ADI-900-020A, Enzo, Farmingdale, NY, USA) as described in the manufacturer's manual. The absorbance was measured at 450nm using a 96-well plate reader (Molecular Devices, FlexStation 3, San Jose, CA, USA).

235

Study Protocols and their Rationale

We used 3 groups of dogs (Figure 1). Group 1 comprised 7 dogs in which coronary stenoses of different degrees were created within the autoregulatory range and eicosanoid levels from the anterior cardiac vein were measured at each stage. Our aim was to determine whether eicosanoids levels changed during decreases in CDP, which would allow us to further explore our hypothesis.

Based on the results from Group 1 dogs we proceeded with experiments in the 28 Group 2 dogs (Figure 1). By then we had access to a specific GPR39 inhibitor, VC108,[15] that had been found to increase CBF in rodents.[16] We created stenoses of varying severities (including flow limiting) in 22 of these dogs to demonstrate the presence of coronary autoregulation, and in 12 of them we collected anterior cardiac venous blood at each stage for metabolomic analysis: adenosine, endothelin-1, polyunsaturated fatty acids (including arachidonic acid and prostaglandins. We then administered VC108 (n=14) or vehicle (n=8) in these animals and added 3 additional dogs to the vehicle group to make the total =11, and measured systemic, pulmonary and coronary hemodynamics 30 min later. Vehicle comprising 10% DMSO was administered as a 5-8 mL IV bolus over 30 s followed by a continuous infusion (120 $mL \cdot hr^{-1}$). Three of these dogs receiving vehicle were used for immunohistochemistry and western blot analysis for GPR39. VC108 suspended in 10% DMSO was administered as a 1.5 mg IV bolus over 30 s followed by a continuous infusion (0.6 $mg \cdot Kg^{-1} hr^{-1}$). This dose was calculated based on >90% receptor occupancy. We then recreated stenoses of varying severities in the 14 dogs receiving VC108 to demonstrate abolishment of coronary autoregulation. Finally, we used 3 additional dogs in which blood levels of VC108 were measured every 10 min for an hour.

Beagle dogs (Group 3) were studied at Aptuit for VC108 pharmacokinetics following daily intravenous administration for 14 days. VC108 was given to 18 dogs (3/sex/group) at 2, 6 and 20 mg/kg once daily for 14 days by intravenous (bolus) administration. Dose volume administered per day was was 2.5 $mL \cdot kg^{-1}$. Pharmacokinetic parameters (drug exposure) were evaluated on Days 1 and 14 (Supplemental data).

At the end of the experiment, with animals still under deep anesthesia, 1 $mL \cdot 4.55\ kg^{-1}$ of Euthasol (sodium pentobarbital 390 $mg \cdot mL^{-1}$ and sodium phenytoin 50 $mg \cdot mL^{-1}$) was administered intravenously in accordance with the June 2020 American Veterinary Medical Association guidelines on euthanasia that is approved by the Institutional Animal Care and Use Committee at our institution.

Immunohistochemistry

After euthanasia, hearts were removed from 3 dogs that had received vehicle during the experiments. Tissues were fixed with fresh 4% paraformaldehyde and cut by cryostat into 20-µm sections that were mounted on superfrost glass slides. After 90 min of blocking in 5% goat serum 1% Bovine Serum Albumin 0.3% Triton-100 in 0.1M PBS at room temperature, sections were labelled with rabbit anti-GPR39 primary antibody (1:50, Invitrogen, #PA5-33709 diluted in blocking buffer) and incubated overnight at 4 °C. The secondary antibody (1:200, Alexa 488-conjugated donkey anti-rabbit (Thermo Fisher Scientific, Cat #A21206)) was diluted in PBS and incubated at room temperature for 2 h. Sections were then stained for 2.5 min with 1:6000 Hoechst 33342 (Thermo Fisher Cat. #62249) and mounted using Fluoromount G® (SouthernBiotech, #0100-01). Digital images of the sections were acquired at 20x with Nikon Imaging System (Nikon Eclipse Tie-A1RSi).

Western Blot

Heart tissues from 3 dogs were homogenized in liquid nitrogen and lysed in RIPA buffer (Thermo Fisher Scientific, Cat. # PI89900) with protease and phosphatase inhibitor (Pierce, Thermo Fisher Scientific, Cat. # A32959). The homogenates were then centrifuged at 14,000 rpm for 20 min at 4°C. The Pierce BCA Protein assay kit (Thermo Fisher Scientific, Cat. # 23225) was used to measure the concentration of protein lysate in samples. Whole heart protein (20 µg per lane) was separated on 4%–12% SDS-polyacrylamide gels and transferred to polyvinylidene difluoride membranes. Total protein staining was performed using Licor Bio Revert® 700 total Protein Stain (Licor Bio, Cat. #926-11016). The membranes were blocked with Licor Intercept® TBS blocking buffer (Licor Bio, Cat. #927-60003) for 60 min at room temperature followed by primary antibodies blocking buffer with 0.02% Tween-20: 1:500 rabbit anti-GPR39 antibody (Novus Biologicals, #NLS139). After 1 h incubation with secondary antibody (IRDye® 800CW Goat anti-Rabbit IgG Secondary Antibody, 1:5000, Licor Bio, Cat. # 926-32211) at room temperature, the membranes were imaged using Licor Odyssey Imager with Image Studio software.

Off-target VC108 Binding

To test off-target VC108 binding, a 131 panel of assays including receptors, enzymes, channels. and transporters was performed at Eurofins Scientific (Luxembourg, Supplemental data).

Statistical Methods

Data were expressed as mean±1 standard error of the mean (SEM). Linear regression as well as repeated measures ANOVA for different stages were used for eicosanoid versus CDP levels in the Group 1 dogs. Comparison of hemodynamic data between vehicle and VC108 in Group 2 dogs was performed using unpaired t test. Comparisons of hemodynamic data between

different stenosis stages prior to and during VC108 administration in the Group 2 dogs was performed using repeated measures ANOVA and subsequent comparison between any 2 stages was performed using t-test with Bonferroni correction. Linear regression was fit to CDP versus all metabolites in 12 Group 2 dogs in which it was measure prior to VC108 administration. Data before and during VC108 administration were compared using 2-way ANOVA. Aggregate CDP versus CBF data in the 22 dogs prior to VC108 administration were fit to a one phase decay function. Linear regression for performed for the aggregate CDP versus CBF data in 14 Group 2 dogs during VC108 administration. Significance was determined at $P<0.05$.

Results

Figure 2 illustrates examples of IHC (A) and western blot (B) of dog heart showing presence of GPR39. Arterioles show GPR39 in green. Nuclei are stained blue. Western blot depicts a characteristic 54 kDa band for GPR39 from 3 different dogs.

Table 1 lists the relation between CDP and all the eicosanoids in 7 Group 1 dogs during 17 stages. Only 15-HETE (vasoconstrictor) showed a significant relation with CDP: As CDP levels decreased so did 15-HETE levels whereas the levels of 14,15-EET (vasodilator) did not change (Figure 3A). Since the ratio of 15-HETE (vasoconstrictor) and 14,15-EET (vasodilator) could influence coronary vascular tone, we determined its relationship with CDP (Figure 3B) and, as expected based on our results, it correlated with CDP.

Since 15-HETE is the endogenous agonist for GPR39,[11] we elected to test the effect of a specific GPR39 antagonist, VC108,[15] on coronary autoregulation. This drug increases CBF in rodents,[16] however, its hemodynamic effects in large animals are unknown. We measured its systemic, pulmonary, and coronary hemodynamics in addition to its effect on coronary autoregulation. Because various vasoactive metabolites have previously been implicated in the

mechanism of coronary autoregulation,[9,10,17-22] we performed comprehensive metabolomics of known coronary vasoactive compounds at different CDPs prior to VC108 administration.

We first created coronary stenoses (including where CDP declined below the autoregulatory range) of the left anterior descending coronary artery in 22 dogs and measured CDP and CBF during each stage (Figure 1). In 12 of these dogs, we sampled 2.5 mL of blood from the anterior cardiac vein for measurement of adenosine, endothelin-1, polyunsaturated fatty acids (including arachidonic acid), and prostaglandins. For prostaglandin and adenosine measurements blood was collected in stop solutions. We then removed the stenosis and allowed coronary hemodynamics to return to normal.

Table 2 lists the systemic and coronary hemodynamics at baseline and during different stenoses stages in 22 dogs (total number of stages = 77). Systemic pressures did not change between stages. In contrast, as expected, CDP decreased with increasing degrees of stenoses and CBF remained constant for non-critical stenoses and declined when stenoses became severe (flow limiting). Constant CBF over a wide range of CDP with non-critical stenosis demonstrates that autoregulation was operative at baseline. MVR decreased progressively with increasing stenoses severity and increased with severe stenosis, although these changes were not statistically significant. We previously reported increased MVR with reduction in resting CBF despite exhaustion of autoregulation caused by a decrease in myocardial blood volume.[23]

Figure 4A illustrates data from individual dogs in the presence of different degrees of coronary stenosis. There is wide variation in baseline CBF between animals depending on the size of the instrumented coronary artery. As a rule, CBF decreased only when CDP was low. Aggregate results from the 22 animals are shown in Figure 4B where autoregulation is clearly

seen with mild and moderate degrees of stenosis, and CBF declined only when CDP was low (severe stenosis). The data fit well to a one phase decay function.

Table 3 depicts the relation between CDP and different metabolites measured from the anterior cardiac vein during different stenosis stages. Only 6-keto-PGF1α, a stable metabolite of prostacyclin (PGI2) that is not vasoactive, showed a significant correlation with CDP. PGI2 itself is quickly metabolized and therefore cannot be measured. It is a vasodilator and its levels should be increased and not decreased at lower CDP. Figure 5 illustrates the relation between CDP and adenosine and endothelin-1, while Figure 6 illustrates the relation between CDP and arachidonic acid and prostaglandins. These cardiac metabolites do not participate in coronary autoregulation.

After collecting these data, we initiated the administration of either VC108 (14 animals) or vehicle (8 animals). We added 3 more dogs to the vehicle group to obtain a comparable number to the VC108 group. Thirty minutes later we measured systemic, pulmonary, and coronary hemodynamics. Table 4 lists the baseline systemic and coronary hemodynamics before administration of VC108 (n=13) or vehicle (n=11). RA pressure was not measured in an additional dog receiving VC108 and data from it are not included in the table. At baseline, prior to administration of either vehicle or VC108, CDP was lower in dogs that were assigned to receive VC108 because of lower mean aortic and consequently distal coronary pressure.

Figure 7 illustrates the change in hemodynamics after VC108/vehicle. There was no difference between VC108 and vehicle in terms of changes in systemic or pulmonary hemodynamics (panels A to E). In comparison, there was a small, albeit non-significant decrease in distal coronary artery pressure (CAP) caused by VC108 compared to vehicle (panel F) accompanied by a significant increase in CBF (panel G) resulting in a significant reduction in the calculated coronary microvascular resistance (MVR, panel H). These results indicate that at

rest inhibition of GPR39 causes reduction in coronary MVR without any change in systemic and pulmonary vascular resistances. No change in cardiac work (product of HR, aortic pressure, left ventricular $\Delta P/\Delta t$) was noted with either vehicle or drug.

We then recreated stenoses of varying severities in the 14 dogs receiving VC108 and measured CDP and CBF at each stage. Table 5 shows results from the different stenosis stages. Systemic pressures did not change between stages. Baseline CBF was higher (26±2 vs. 19±2 $mL.min^{-1}$, p=0.05) and MVR was lower (2.42±0.20 vs. 3.58±0.27 $mmHg{\cdot}mL^{-1}{\cdot}min^{-1}$, p=0.03) during VC108 compared to prior to VC108 (Table 2). The increase in CBF compared to baseline was less than the maximal increase in CBF noted after 20 s coronary occlusion at the beginning of the experiment indicating that VC108 does not maximally dilate coronary arterioles. CBF declined with each level of non-critical stenosis, indicating abolishment of coronary autoregulation. Because of coronary vasodilation caused by VC108, MVR remained similar during all levels of non-critical coronary stenosis but increased when the stenosis was critical. We previously showed that the majority (>75%) of increase in MVR distal to critical stenosis during coronary vasodilation occurs from capillary derecruitment distal to stenosis.[23]

Figure 4C illustrates results from the 14 individual dogs where different degrees of stenoses were placed in the presence of intravenously administered VC108. As a rule, CBF decreased with decreasing CDP, although the slopes of the decline and baseline CBF varied between animals. Aggregate results of the 74 stages from 14 animals are shown in Figure 4D. There is a linear relation between CDP and CBF implying that VC108 abolishes autoregulation.

Table 6 illustrates the results of 2-way ANOVA comparison of systemic and coronary hemodynamics during various degrees of stenosis in the absence (Table 2) or presence (Table 5)

of VC108. Except for RA pressure, the interactions between each variable are highly significant, indicating that the conditions were independent of each other.

In 3 naïve dogs we administered VC108 and measured drug levels every 10 min for one hour (Table 7). The elevated level at 10 min is from the bolus injection (see methods), after which the drug level remains steady during VC108 infusion. The mean blood/plasma ratio from 3 animals was 0.98. Of note, the ratio of free plasma concentration/IC50 of VC108, which in the dog is 31.6 nM, is well over unity, implying therapeutic effect. Of the 131 receptors, channels, and enzymes studied for off-target binding, VC108 did not bind to any of them (Supplemental data).

In addition, the 18 Group 3 beagle dogs (9 female and 9 male) were administered daily intravenous bolus injections of VC108 at 3 different doses (2, 6, and 20 $mg \cdot kg^{-1}$) and pharmacokinetics were determined at days 1 and 14. There was no difference in drug exposure between female and male dogs at all 3 doses both on day 1 and day 14 (Supplemental data).

Discussion

Using a comprehensive metabolomic analysis of vasoactive molecules that could have a putative role in coronary autoregulation, we show for the first time that coronary venous levels of 15-HETE, the endogenous agonist of GPR39, is the only molecule that correlates meaningfully to changes in CDP, whereas other vasoactive metabolites do not. Since 15-HETE acts through GPR39, our results indicate that GPR39 is the molecular switch that controls coronary vasomotion. This is supported by the finding that after administration of VC108, a specific GPR39 inhibitor, coronary MVR decreased. In the absence of VC108, CBF remained constant over a wide range of CDPs induced by varying degrees of coronary stenosis indicating intact autoregulation. VC108 abolished coronary autoregulation so that CBF became CDP dependent.

Therefore, GPR39 and its endogenous agonist 15-HETE together orchestrate coronary autoregulation.

In our previous study, where we showed that GPR39 was the receptor for the endogenous ligands 15-HETE and 14,15-EET in the mouse, we stripped the heart of all large vessels and demonstrated the presence of GPR39 on VSMCs in the coronary microvasculature using immunohistochemistry: GPR39 was present in coronary resistance arterioles[11], similar to results from our current study in dogs. In addition, we showed the presence of GPR39 in mouse heart using western blot[11], similar to results from our current study in dogs. Using a mouse Langendorf constant flow preparation we showed that 15-HETE increased CDP above the normal range, an effect that was abolished in GPR39 knockout mice. In these experiments, 14,15-EET alone had no effect on CDP. Our current results extend these observations.

GPR39 exhibits constitutive activity through Gαq and Gα12/13, which may explain its role in maintaining resting coronary vascular tone.[24,25] Zn^{++} serves as an allosteric modulator of GPR39.[24,25] In the presence of Zn^{++}, GPR39 activation by 15-HETE leads to extracellular signal-regulated kinase (ERK) phosphorylation and intracellular Ca^{++} mobilization,[11] suggesting activation of G-protein αq (Gαq). Increased intracellular Ca^{++} results in VSMC contraction. The higher the level of 15-HETE, the greater the stimulation of GPR39 and the greater the intracellular Ca^{++} and consequent vasoconstriction.[11] As 15-HETE levels decrease the reverse occurs, leading to less intracellular Ca^{++} and less vasoconstriction (or more vasorelaxation). In the intact animal changes in CDP can occur moment to moment requiring a corresponding change in CBF. Therefore, from a systems perspective it seems efficient to have one molecule act on one receptor to affect instant changes, akin to a thermostat rather than an off/on switch. The very short plasma half-life of 15-HETE supports this notion.

Role of Arachidonic acid Metabolites

Prostaglandins, another set of arachidonic acid derivatives, were examined previously where administration of two inhibitors of prostaglandin synthesis (5,9,11,14-eicosatetraynoic acid and indomethacin) abolished coronary autoregulation in the perfused isolated rabbit heart,[26] although studies in larger animals did not show any effects of indomethacin on CBF.[27,28] The same investigators who reported the effect of prostaglandin synthesis inhibition in the isolated rabbit heart subsequently reported an 'active' substance, an unidentified albumin bound lipid molecule, that counteracted the effects of indomethacin.[29] Although it cannot be definitively proven, our results suggest that this 'active' substance could have been 15-HETE, a metabolite of arachidonic acid, which the investigators did not measure. When human endothelial cells are stimulated by histamine, they enhance synthesis of both prostaglandin and 15-HETE.[30] Both are inhibited by indomethacin, which might explain why autoregulation was abolished with the drug in the perfused isolated rabbit heart.[31] Our results indicate that prostaglandins, specifically TBXA2, PDE2, PGE2, and $PGF2_{\alpha}$, do not participate in autoregulation. We saw a mild decline in the prostacyclin metabolite 6-keto-PGF1α, which is not vasoactive.

Of the eicosanoids, another group of arachidonic acid metabolites, only 15-HETE showed a significant correlation with CDP in our study. However, a borderline correlation between CDP and 12-HETE was also noted. Both 15- and 12-HETE are produced by the same enzyme (12/15LOX) and their ratio depends on the species. In our study the 12-HETE/15-HETE ratio was approximately 20:1. The main receptor for 12-HETE is GPR31, which is thought not to be present in VSMCs.[22] We previously reported that 12-HETE had no effect on GPR39.[11] 12-HETE is a competitive thromboxane A2 receptor antagonist, which would make it a vasodilator although its action on VSMCs is complex and controversial.[22] Coronary venous plasma levels of

arachidonic acid itself remained unchanged at different CDPs, indicating that changes in coronary pressure influenced arachidonic acid to 15-HETE conversion by 12/15 LOX probably by release of more substrate from the lipid bilayer by phospholipase A_2.

Role of Other Pathways-Comparison with Previous Studies

Nitric oxide (NO) has been implicated in coronary autoregulation.[17] There are several pathways through which GPR39, 15-HETE, and NO interact with each other to explain these findings. First, increased intracellular Ca^{++} stimulates endothelial NO synthetase (eNOS) resulting in increased NO production.[32] NO, in turn, stimulates sarcoplasmic endoplasmic reticulum Ca^{++}ATPase, thereby increasing Ca^{++} reuptake into sarcoplasmic endoplasmic reticulum and decreasing vascular tone.[33] GPCRs can undergo post-translation modification induced by S-nitrosylation whereby NO could modify the response of GPR39 to 15-HETE in vivo.[34] Thus, inhibition of eNOS by NG-nitro-L-arginine would interfere with autoregulation as previously reported[17] by inhibiting signaling both at the level of GPR39 and downstream to it. However, we did not test this possibility in our current study.

Inhibition of α-adrenergic systemic has been shown to alter coronary autoregulation.[18] α-adrenergic stimulation causes increased production of arachidonic acid through activation of mitogen-activated protein kinases that are downstream to ERK, enhancing arachidonic acid production from the nuclear envelope.[35] It also increases production of arachidonic acid and its metabolites by increasing intracellular Ca^{++}, which stimulates cytosolic phospholipase (PLA_2) production that is responsible for release of arachidonic acid from plasma membrane.[36] Thus, α-adrenergic inhibition by drugs such as prazocin reported previously[18] could affect coronary autoregulation through inhibition of arachidonic acid and 15-HETE production, mechanisms proximal to GPR39.

Vasodilation requires VSMC hyperpolarization that is mediated through increased levels of intracellular K^+ resulting from K^+ channel opening.[19] 15-HETE directly inhibits K^+ channel activity, thus attenuating vasodilation.[37] Lower levels of 15-HETE seen with coronary arteriolar

vasodilation at lower CDPs are therefore likely associated with more active K^+ channels that are open and allow intracellular K^+ flux under appropriate circumstances. Open K^+ channels-induced hyperpolarization also decreases Ca^{++} sensitivity.[38] Other K^+ channel blockers have also been associated with disruption of coronary autoregulation.[10,20,39] H_2O_2 opens Ca^{++} gated and voltage-dependent K^+ channels allowing VSMC hyperpolarization.[39] Therefore, K^+ channel blockers like tetraethyl ammonium and 4-aminopyridine block the effect of H_2O_2, thus interfering with vasodilation.[20] A similar explanation can be provided for attenuation of coronary autoregulation by glibenclamide, an ATP-sensitive K^+ channel blocker.[20] K^+ channel activity is downstream to GPR39 activation.

Finally, adenosine was previously shown not to participate in coronary autoregulation[9,10] and we confirmed the finding. Additionally, we show that endothelin-1, a potent coronary vasoconstrictor[40] also does not participate in coronary autoregulation.

Proposed Mechanism of Coronary Autoregulation

Based on our results we propose the following scenario for coronary autoregulation shown in the central illustration. Changes in CDP are mechanosensed by ion channels[41,42] or G-protein coupled receptors[43-45] present on VSMCs, which then either activate PLA_2 to release the substrate arachidonic acid from plasma membrane to produce its metabolites or directly modulate 12/15 LOX activity resulting in 15-HETE production. 15-HETE then activates GPR39, which in turn causes intracellular Ca^{++} release resulting in VSMC contraction. Higher CDP causes higher 15-HETE production and more vasoconstriction while lower CDP causes less 15-HETE production and less vasoconstriction (or relative vasodilation). Counterintuitively, no vasodilators actively participate in this process. Coronary vascular tone needs to be rapidly adjusted to myocardial oxygen needs or CDP changes, implying that the molecular switch for

coronary autoregulation needs to act more like a thermostat than a lock and key, which is readily accomplished by a single biomolecule acting on a single receptor. Having the same receptor detect changes in ambient arteriolar pressure would make the autoregulatory circuit more efficient.

Limitations of our Study

Sex differences are well known to affect coronary vascular reactivity in dogs.[46,47] Uncertainty of the time during the ovulation cycle or possible pregnancy, prevented us from using female dogs. Thus, our results cannot be extrapolated to females in terms of vascular reactivity at baseline and during VC108 administration. In terms of exposure of animals to VC108 dose we found that both sexes of Beagle dogs had equal exposure to the drug.

Anesthesia can also affect coronary vascular reactivity. Although there are no direct interactions reported between the combination of hydromorphone, ketamine, and midazolam with arachidonic acid metabolism and GPR39 activation, ketamine indirectly modulates the arachidonic acid pathway by inhibiting the N-methyl-D-aspartate receptor-mediated calcium influx[48], resulting in reduced phospholipase A_2 activity and arachidonic acid release. However, this effect likely did not confound our results as arachidonic acid levels remained unchanged throughout the range of CDP that was studied.

We did not study the upper range of autoregulation (100-120 mm CDP). Nonetheless, based on our previous results using a constant flow Langendorff mouse model,[11] we predict that increasing CDP above the normal range would increase 15-HETE levels and cause further vasoconstriction to maintain constant CBF. In the dog, intracoronary injection of 15-HETE causes CBF decline from increased MVR that is mitigated by pre-treatment with VC108.[49] We did not see elevation of adenosine or endothelin-1 levels at low CDP probably because ischemia

was not produced due to adequate collateral flow to the myocardial region supplied by the left anterior descending artery. Collateral blood flow is high in the dog.[50]

While 15-HETE is the main metabolite that showed a correlation with CDP, the r^2 value is <50 with significant scatter, which may be related to collateral blood flow, variability in coronary anatomy between dogs, and measurement variability. In addition, since CBF is highly regulated other redundant and overlapping factors (neural, metabolic, etc.) may contribute to coronary autoregulation.

We did not measure cardiac metabolite levels during VC108 administration because in our early experiments we noted hemolysis after centrifugation of the coronary venous blood samples. It was then determined that hemolysis was caused by DMSO.[51]

Conclusion

In this study we show for the first time that 15-HETE participates in the resting coronary vascular tone in dogs. We also demonstrate that 15-HETE acting through GPR39 is responsible for coronary autoregulation when CDP is reduced. Factors that have previously been described to effect coronary autoregulation either modify GPR39 directly or act through signaling pathways upstream or downstream of GPR39. Hence, GPR39 serves as the molecular switch responsible for coronary autoregulation.

Author Contributions

Drs. Le and Kaul developed the concept and design for the studies. They also wrote the manuscript. Drs. Kajimoto and Zhao participated in the studies and performed the surgery and delivered anesthesia and drugs. Dr. Methner performed ELISA for endothelin-1, western blot for GPR39, and prepared VC108 bolus and infusions. Dr. Cao performed immunohistochemistry. Dr. Le analyzed the data and created the tables and figures. Drs. Cianciulli, Semeraro, Trist and Micheli contributed to the development of VC108. Drs. Franchi, Marcheselli, and Parazzoli performed the pharmacokinetic studies in beagle dogs.

Acknowledgements

Metabolomic analysis was performed by the Bioanalytical Shared Resource/ Pharmacokinetics Core Facility, which is supported in part by the University Shared Resource Program at Oregon Health and Sciences University. Special thanks to Lisa Byle and Jenny Luo for the analysis. We are also grateful to Joseph Sciurba DVM and his team in the department of comparative medicine for their participation in the study and care of the animals.

The research reported in this publication used computational infrastructure supported by the Office of Research Infrastructure Programs, Office of the Director, of the National Institutes of Health under Award Number S10OD034224. The content is solely the responsibility of the authors and does not necessarily represent the official views of the National Institutes of Health.

Conflict of Interest

Oregon Health & Science University and Vasocardea, Inc. have a joint patent application filed globally (see WO2021222858 and corresponding national filings) that encompasses drugs that inhibit GPR39. Vasocardea, Inc. has an additional patent application filed globally (see WO2023076219 and corresponding national filings) that encompasses VC108. Vasocardea, Inc. has exclusive rights to develop and commercialize drugs under all of these patent applications. Evotec has assigned all patent rights to Oregon Health & Science University and Vasocardea, Inc.

Dr. Kaul is the founder and President of Vasocardea, Inc., a Delaware incorporated company located in Portland, Oregon.

The information in this manuscript does not represent the views of the Veterans Administration or the US government.

References

1. Mosher P, Ross J Jr., McFate PA, Shaw RF. Control of coronary blood flow by an autoregulatory mechanism. *Circ Res* 1964;16:250-259.
2. Rouleau J, Boerboom LE, Surjadhana J, Hoffman JIE. The role of autoregulation and tissue diastolic pressures in the transmural distribution of left ventricular blood flow in anesthetized dogs. *Circ. Res.*1979;45:804–815.
3. Kanatsuka H, Lamping KG, Eastham CL, Marcus ML. Heterogeneous changes in epimyocardial microvascular size during graded coronary stenosis. Evidence of the microvascular site for autoregulation. *Circ Res*. 19900;66, 389–396.
4. Dick GM, Namani R, Patel B, Kassab GS. Role of coronary myogenic response in pressure-flow autoregulation in swine: A meta-analysis with coronary flow modeling. *Frontiers in Physiology* 2018;10.3389/ fphys. 2018. 00580/full.
5. Starling, EH. On the Absorption of Fluids from the Connective Tissue Spaces. *J Physiol*. 1896;19:312-326.
6. Deussen A. Mechanisms underlying coronary autoregulation continue to await clarification. *Basic. Res. Cardiol.* 2018;113:33-34.
7. Gebremedhin D, Lange AR, Lowry TF, Taheri R, Birks EK, Hudetz AG, Narayanan J, Falck JR, Okamoto H, Roman RJ, Nithipatikom K, Campbell WB, Harder DR. Production of 20-HETE and Its Role in Autoregulation of Cerebral Blood Flow. *Circ. Res.* 2000;87:60-65.
8. Smith WL. The eicosanoids and their biochemical mechanisms of action. *Biochem. J.* 1989;259: 315-324.

9. Hanley FL, Grattan MT, Stevens MB, Hoffman JIE. Role of adenosine in coronary autoregulation. *Am. J. Physiol.* 1986;250:H558-H566.

10. Stepp DW, Kroll K, Feigl EO. K^+ATP channels and adenosine are not necessary for coronary autoregulation. *Am. J. Physiol*. 1997;273:H1299–H1308.

11. Alkayed NJ, Cao Z, Qian ZY, Nagarajan S, Liu X, Nelson J, Xie F, Li B, Fan W, Xiao X, Barnes AP, Kaul S. Control of Coronary Vascular Resistance by Eicosanoids via a Novel GPCR. *Am. J. Physiol.* 2022;322:C1011-C1021.

12. Dumlao DS, Buczynski MW, Norris PC, Harkewicz R and Dennis EA. High-throughput lipidomic analysis of fatty acid derived eicosanoids and N-acylethanolamines. *Biochim Biophys Acta* 2011;1811:724-736.

13. Sharma K, Singh R, Giri S, Rajagopal S and Mullangi R. Highly sensitive method for the determination of adenosine by LC-MS/MS-ESI: method validation and scope of application to a pharmacokinetic/pharmacodynamic study. *Biomed Chromatogr* 2012; 26:81-88

14. Shryock JC, Boukin MT, Hill JA, Belardinelli L. A new method of sampling blood for measurement of plasma adenosine. *Am J Physiol* 1990;258:H1232-H1239.

15. Cianciulli A, Bernadelli A, Faedo S, Le E, Methner C, Pellacani A, Semeraro T, Trist ILM, Kaul S, Micheli F. Identification of Novel and selective GPR39 receptor antagonists for the treatment of Acute Myocardial Ischemia. Chem Med Chem 2025; https://doi.org/10.1002/cmdc.202500662

16. Methner C, Le DE, Kaul S. Targeting GPR39 for no reflow after acute myocardial infarction. *Circulation* 2023;148 (Suppl_1):18781.

17. Ueeda M, Silvia SK, Olsson RA. Nitric oxide modulates autoregulation in guinea pigs. *Circ. Res.* 1992;70:1296-1303.

18. Jones CE, Liang IYS, Gwirtz PA. Effect of α-adrenergic blockage on coronary autoregulation in dogs. *Am. J. Physiol.* 1987;253:H365-H372.

19. Jackson WF. Potassium Channels in regulation of vascular smooth muscle contraction and growth. *Adv. Pharmacol*. 2017;78:89-144

20. Yada T, Shimokawa H, Hiramatsu O, Kajita T, Shigeto F, Goto M, Ogasawara Y, Kajiya F. Hydrogen peroxide, an endogenous endothelium-derived hyperpolarizing factor, plays an important role in coronary autoregulation in vivo. *Circulation.* 2003;107:1040-1045.

21. Narishige T, Egashira K, Akatsuka Y, Katsuda Y, Numaguchi K, Sakata M, Takeshita A. Glibenclamide, a putative ATP-Sensitive K^+ channel blocker, inhibits coronary autoregulation in anesthetized dogs. *Circ. Res.* 1993;73:771-776

22. Pascale JV, Lucchesi PA, Garcia V. Unraveling the Role of 12- and 20- HETE in Cardiac Pathophysiology: G-Protein-Coupled Receptors, Pharmacological Inhibitors, and Transgenic Approaches. *J Cardiovasc Pharmacol*. 2021;77:707-717.

23. Jayaweera AR, Wei K, Coggins M, Bin JP, Goodman C, Kaul S. Role of capillaries in determining coronary blood flow reserve: New insights using myocardial contrast echocardiography. *Am J Physiol* 1999;277:H2363-H2372.

24. Holst B, Egerod KL, Schild E, Vickers SP, Cheetham S, Gerlach L-O, Storjohann L, Stidsen CE, Jones R, Beck-Sickinger AG, Schwartz TW. GPR39 signaling is stimulated by zinc ions but not by obestatin. *Endocrinology* 148:13–20.

25. Storjohann L, Holst B, Schwartz TW. Molecular mechanism of Zn^{2+} agonism in the extracellular domain of GPR39, *FEBS Letters*, 2008;582.

26. Moretti RL, Abraham S, Ecker RR. The stimulation of cardiac prostaglandin production by blood plasma and its relationship to the regulation of coronary flow in isolated isovolumic rabbit hearts. *Circ. Res.* 1976;39:231-238.

27. Rubio R, Berne RM. Regulation of coronary blood flow. *Prog. Cardiovasc. Dis.* 1975;18:105-122.

28. Dai XJ, Bache RJ. Effect of indomethacin on coronary blood flow during graded treadmill exercise in the dog *Am. J. Physiol*. 1984:247:H452-H458.

29. Moretti RL, Abraham S. Stimulation of microsomal prostaglandin synthesis by a blood plasma constituent which augments autoregulation and maintenance of vascular tone in isolated rabbit hearts. *Circ. Res.* 1978;42:317-323.

30. Revtyak GE, Hughes MJ, Johnson AR, Campbell WB. Histamine stimulation of prostaglandin and HETE synthesis in human endothelial cells. *Am. J. Physiol.* 1988;255(2 Pt 1):C214-225.

31. Salari H, Braquet P, Borgeat P. Comparative effects of indomethacin, acetylenic acids, 15-HETE, nordihydroguaiaretic acid and BW755C on the metabolism of arachidonic acid in human leukocytes and platelets. *Prostaglandins Leukotrienes and Medicine* 1984;13:53-60.

32. Fleming I, Busse R. Signal transduction of eNOS activation. *Cardiovasc. Res.* 1999;43:532–541.

33. Tong X, Evangelista A, Cohen RA. Targeting the redox regulation of SERCA in vascular physiology and disease. *Curr. Opin. Pharmacol*. 2010;10:133-138.

34. Daaka Y. S-Nitrosylation-regulated GPCR signaling. *Biochim. Biophys. Acta*. 2012; 1820:743–751.

35. Burch RM, Luini A, Mais DE, Corda D, Vanderhoek JY, Kohn LD, Axelrod J. Alpha 1-adrenergic stimulation of arachidonic acid release and metabolism in a rat thyroid cell line. Mediation of cell replication by prostaglandin E2. *J Biol. Chem*. 1986;261:11236-11241.

36. Nebigil C, Malik KU. Alpha adrenergic receptor subtypes involved in prostaglandin synthesis are coupled to Ca^{++} channels through a pertussis toxin-sensitive guanine nucleotide-binding protein. *J. Pharmacol. Exp. Ther.* 1993;266:1113-1124.

37. Li Y, Li Q, Wang Z, Liang D, Liang S, Tang X, Guo L, Zhang R, Zhu D. 15-HETE suppresses K(+) channel activity and inhibits apoptosis in pulmonary artery smooth muscle cells. *Apoptosis*. 2009;1:42-51.

38. Gutterman DD, Miura H, Liu Y. Redox modulation of vascular tone. Focus of potassium channel mechanisms of dilation. *Arterioscl. Thromb. Vasc. Biol.* 2005;25:671–678.

39. Nacitarhan C, Bayram Z, Eksert B, Usta C, Golbasi I, Ozdem SS. The Effect of hydrogen peroxide in human internal thoracic arteries: role of potassium channels, nitric oxide and cyclooxygenase products. *Cardiovasc. Drugs. Ther*. 2007;21:257–262

40. Teerlink JR, Breu V, Sprecher U, Clozel M, Clozel JP. Potent vasoconstriction mediated by endothelin ETB receptors in canine coronary arteries. *Circ Res*. 1994; 74:105-114..

41. Hardie RC. TRP channels and lipids: from Drosophila to mammalian physiology. *J Physiol* 2007;578:9-24.

42. Munaron L. Shuffling the cards in signal transduction: Calcium, arachidonic acid and mechanosensitivity. *World. J. Biol. Chem.* 2011;2:59-66.

43. Erdogmus S, Storch U, Danner L, Becker J, Winter M, Ziegler N, Wirth A, Offermanns S, Hoffmann C, Gudermann T, Mederos y Schnitzler M, Helix 8 is the essential structural motif of mechanosensitive GPCRs. *Nat Commun* 2019;10:5784.

44. Hardman K, Goldman A, Pliotas C. Membrane force reception: mechanosensation in G protein-coupled receptors and tools to address it. *Curr. Op. Physiol*. 2023;35: 100689.

45. Cullum SA, Platt S, Dale, N, Isaac OC, Wragg ES, Soave M, Veprintsev DB, Woolard J, Kilpatrick LE, Hill SJ.. Mechano-sensitivity of β2-adrenoceptors enhances constitutive activation of cAMP generation that is inhibited by inverse agonists. *Commun Biol* 2024;7:417.

46. Karanian J; Ramwell P. Effect of Gender and Sex Steroids on the Contractile Response of Canine Coronary and Renal Blood Vessels. *J. Cardiovasc. Pharmacol*. 1996;27: 312-319.

47. Wellman GC, Bonev AD, Nelson MT, Brayden JE. Gender differences in coronary artery diameter involve estrogen, nitric oxide, and Ca(2+)-dependent K+ channels. *Circ. Res.* 1996;79:1024-1030.

48. Orser BA, Pennefather PS, MacDonald JF. Multiple mechanisms of ketamine blockade of N-methyl-D-aspartate receptors. *Anesthesiology*. 1997;86:903-917.

49. Le DE, Kajimoto M, Zhao Y, Methner C, Kaul S. VC108, a GPR39 blocker, increases coronary blood flow and inhibits the vascular effects of 15-hydroxyeicosatetraenoic acid. Circulation 152 (suppl_3):4357647, 2025.

50. Schaper W, Binz K, Sass S, Winkler B. Influence of collateral blood flow and of variations in MV□O2 on tissue-ATP content in ischemic and infarcted myocardium. *J. Mol. Cell. Cardiol.* 1987;19:19-37.

51. Yi X, Liu M, Luo Q, Zhuo H, Cao H, Wang J, Han Y. Toxic effects of dimethyl sulfoxide on red blood cells, platelets, and vascular endothelial cells *in vitro*. *FEBS Open Bio*. 2017;7:485-494.

Table 1. Relation between Coronary Driving Pressure and Coronary Venous Eicosanoid Levels (n=7 dogs, 17 stages)

Eicosanoid Isomer	Linear Regression Equation	Linear regression R^2	Linear Regression p value	Repeated Measures ANOVA P value
5,6-EET	y = 0.9392x + 42.17	0.0758	0.3902	0.5021
8,9-EET	y = 0.0273x + 40.01	0.0005	0.9338	0.1321
11,12-EET	y = 0.0843x + 31.53	0.0206	0.3376	0.0823
14,15-EET	y = 0.0911x + 48.96	0.0063	0.7626	0.3248

5,6-DHET	y = -0.0957x + 37.02	0.0143	0.6481	0.7946	
8,9-DHET	y = -0.0230x + 51.04	0.0009	0.9106	0.9770	
11,12-DHET	y = -0.2599x + 132.6	0.0192	0.5955	0.9821	
14,15-DHET	y = -0.1528x + 104.6	0.0086	0.7240	0.9948	
11-HETE	y = 2.7060x + 15.70	0.0316	0.4950	0.3528	
12-HETE	y = 44.94x + 129.10	0.2308	0.0596	0.4142	
15-HETE	y = 3.0350x + 4.7770	0.4700	0.0024	0.0104	
20-HETE	y = -5.523x + 1964	0.0188	0.5994	0.7959	

Parameter	Baseline (n=22)	Mild Stenosis Gradient ≤10 mmHg	Moderate Stenosis Gradient 11 – 34 mmHg	Severe Stenosis Gradient ≥35 mmHg	p value Anova

Table 2. Systemic and Coronary Hemodynamics for 22 Protocol 3 Dogs at Baseline and Varying Degrees of Coronary Stenosis (n=77 Stages) Prior to VC108 Administration (mean ± SEM)

		(n=19)	**(n=28)**	**(n=8)**	
Heart rate (bpm)	97±3	93±3	96±3	104±3	0.3023
Mean blood pressure (mmHg)	74±3	71±2	70±1	64±4	0.2897
Right atrial blood pressure (mmHg)	12±1	12±1	12±1	13±1	0.7037
Mean distal coronary artery pressure (mmHg)	74±3*‡□	65±2‡□	55±2□	35±3	<0.0001
Coronary artery driving pressure (mmHg)	63±3*‡□	53±2†□	43±2□	22±3	<0.0001
Coronary artery blood flow ($mL \cdot min^{-1}$)	19±2□	17±1□□	17±1□	9±1	0.0002
Coronary microvascular resistance ($mmHg \cdot mL \cdot min^{-1}$)	3.58±0.27	3.52±0.31	2.88±0.28	3.14±0.45	0.2607

*$p < 0.05$ v. mild stenosis gradient
†$p < 0.05$ v. moderate stenosis gradient
‡$p < 0.0001$ v. moderate stenosis gradient
□$p < 0.01$ v. severe stenosis gradient
□$p < 0.0001$ v. severe stenosis gradient

Table 3. Relation between Coronary Driving Pressure and Cardiac Venous Metabolite Levels During Baseline and Various Stenosis Stages Prior to VC108 Administration in 12 Dogs

Metabolite (pg/mL)	Equation	r^2	p value
Adenosine (n=49)	y = 0.2641x + 28.78	0.0201	0.3309
Endothelin (n=49)	y = -0.0066x + 9.94	0.0001	0.9340
Prostaglandins			
6-keto Prostaglandin (n=46)	y = 1.570x + 77.28	0.0992	0.0330
Thromboxane 2 (n=46)	y = 11.79x + 8.53	0.0502	0.1345
Prostaglandin E2 (n=48)	y = 0.2014x + 27.46	0.0195	0.3435
Prostaglandin D2 (n=48)	y = 0.1326x + 23.56	0.0047	0.6420
Prostaglandin $F2_{\alpha}$ (n=49)	y = 0.3365x + 41.22	0.0047	0.6390
Polyunsaturated Fatty Acid			
Arachidonic acid (n-49)	y = -0.1259x + 416.50	0.0008	0.8454
Oleic Acid (n=49)	y = 0.2577x + 146.90	0.0071	0.5652
Linolenic Acid (49)	y = 0.0051x + 0.0019	0.0019	0.7642
Gama Linoleic Acid (n=49)	y = 0.0209x + 5.10	0.0349	0.1988
Linoleic Acid (n=49)	y = 0.0418x + 478.20	0.0022	0.7491
Eicosapentaenoic Acid (n=49)	y = 0.0133x + 5.19	0.0212	0.3185
Docosahexanoic Acid (n=49)	y = -0.0369x + 29.64	0.0029	0.7132

Hemolyzed samples not analyzed

Table 4. Baseline Systemic and Coronary Hemodynamics in Protocol 2 Dogs Prior to Vehicle/Drug Administration (mean ± SEM)

Parameter	Vehicle (n=11)	VC108 (n=13)	p value
Heart rate (bpm)	101±6	104±3	0.6092
Mean aortic pressure (mmHg)	80±5	72±2	0.1048
Mean right atrial pressure (mmHg)	11±2	12±1	0.5283
*Left ventricular $\Delta P/\Delta t$ ($mmHg \cdot s^{-1}$)	1082±185	868±127	0.3533
*Mean pulmonary artery pressure (mmHg)	23±5	16±1	0.1461
Distal coronary artery pressure (mmHg)	82±4	72±2	0.0508
Coronary artery driving pressure (mmHg)	71±4	60±2	0.0108
Coronary artery blood flow ($mL \cdot min^{-1}$)	21±2	22±2	0.9097
Coronary microvascular resistance ($mmHg \cdot mL^{-1} \cdot min^{-1}$)	3.66±0.49	3.14±0.30	0.3747

*Measured in 6 dogs

Table 5. Systemic and Coronary Hemodynamics for 14 Protocol 3 Dogs at Baseline and with Varying Degrees of Coronary Stenoses (n=74 stages) During VC108 Administration (mean ± SEM)

Parameter	Baseline (n=14)	Mild Stenosis Gradient ≤10 mmHg (n=10)	Moderate Stenosis Gradient 11 – 34 mmHg (n=32)	Severe Stenosis Gradient ≥35 mmHg (n=18)	p value Anova
Heart rate (bpm)	104±3	104±3	108±2	106±2	0.6373
Mean blood pressure (mmHg)	71±2	76±3	75±2	76±2	0.3918
Right atrial blood pressure (mmHg)	13±0	13±0	13±0	13±0	0.4900
Mean distal coronary artery pressure (mmHg)	71±2‡□	70±3‡□	56±1□	40±1	<0.0001
Coronary artery driving pressure (mmHg)	59±2‡□	56±3‡□	43±1□	27±2	<0.0001
Coronary artery blood flow ($mL \cdot min^{-1}$)	26±2□	22±2□	20±2□	8±1	<0.0001
Coronary microvascular resistance ($mmHg \cdot mL \cdot min^{-1}$)	2.42±0.20¥	2.64±0.22□	2.56±0.16□	4.63±0.59	<0.0001

*$p < 0.05$ v. mild stenosis gradient
†$p < 0.05$ v. moderate stenosis gradient
‡$p < 0.0001$ v. moderate stenosis gradient
□$p < 0.01$ v. severe stenosis gradient
¥$p < 0.001$ v. severe stenosis gradient
□$p < 0.0001$ v. severe stenosis gradient

Table 6. 2-Way ANOVA interactions between variables in Tables 5 and 6 (Protocols 3 Dogs)

Parameter	F value	p value
Heart rate (bpm)	21.22	<0.0001
Mean blood pressure (mmHg)	52.22	<0.0001
Right atrial blood pressure (mmHg)	0.98	0.4011
Mean distal coronary artery pressure (mmHg)	25.25	<0.0001
Coronary artery driving pressure (mmHg)	23.65	<0.0001
Coronary artery blood flow ($mL \cdot min^{-1}$)	30.55	<0.0001
Coronary microvascular resistance ($mmHg \cdot mL \cdot min^{-1}$)	86.41	<0.0001

Table 7. Total and Free Blood Concentrations (nM) as well as 1C50/Free Blood Concentration of VC108 After a 1.5 mg Bolus Injection Followed by 0.6 mg/kg/h Infusion in 3 Protocol 1 Dogs

Time After Administration (min)	Total Blood Concentration	Free Blood Concentration	Free Plasma Concentration	Free Plasma Concentration/IC50
10	14752 (4054-31573)	4661	4568	71
20	6824 (5234-8710)	2156	2113	33
30	6382 (4664-8700)	2017	1977	31
40	5876 (3900-8348)	1857	1820	28
50	6094 (3618-10297)	1926	1887	29
60	5902 (3767-8974)	1653	1620	25

Blood plasma ratio of VC108=0.98
IC50 of VC108=31.6 nM

Figure Legends

Figure 1: Breakdown of the animals used in the study and protocols they underwent. Created in https://Biorender.com. IHC=immunohistochemistry; WB=western blot.

Figure 2: Examples of IHC (A) and western blot (B) of dog heart showing presence of GPR39. GPR39 (in green) is seen lining the arterioles (A). Nuclei are stained blue (DAPI). Western blot depicts a characteristic 54 kDa band for GPR39 from 3 different dogs. GPR39=G-protein coupled receptor, 39; DAPI=4′,6-diamidino-2-phenylindole

Figure 3: Relation between coronary driving pressure and anterior cardiac venous plasma levels of A)15-HETE and 14,15-EET from 7 dogs undergoing different degrees of coronary stenosis within the autoregulatory range, and B) 15-HETE/14,15-EET ratio. 15-HETE=15-hydroxyeicosatetraenoic acid; 14,15-EET=14,15-epoxyeicosatrienoic acid.

Figure 4: Coronary driving pressure versus coronary artery blood flow results from protocols 2 and 3. A) Data from 22 individual dogs (77 unique stages) in the absence of VC108 showing flat coronary artery blood flow over a wide range of coronary driving pressures, with decreasing flow at low coronary driving pressures. B) Aggregate results from the same animals as in panel A, showing classical coronary autoregulation over a wide range of coronary driving pressures with a decline in coronary artery flow at low coronary driving pressures. Data were fit using one phase decay least-squares analysis. C) Data from 14 of the 22 individual dogs (74 unique stages) from protocol 2 in the presence of VC108 (protocol 3) showing declining coronary artery blood flow with lowering of coronary driving pressure. D) Aggregate results from the same animals as in panel C, showing abolishment of coronary autoregulation with coronary artery blood flow becoming coronary driving pressure dependent. Data were fit using linear regression analysis.

Figure 5: Relation between coronary driving pressure and anterior coronary vein plasma concentrations of A) adenosine and B) endothelin-1 from 12 dogs undergoing various degrees of coronary stenoses at rest.

Figure 6: Relation between coronary driving pressure and anterior coronary vein plasma concentrations of A) Arachidonic acid; B) 6-keto-PGF_{α}, (an inactive metabolite of prostaglandin I2; C) Thromboxane A2; D) Prostaglandin E2; E) Prostaglandin D2; and F) Prostaglandin $F2_{\alpha}$.

Figure 7: Percent change from baseline in systemic, pulmonary, and coronary hemodynamics with administration of Vehicle (VEH, n=11) or VC108 (n=13). A) HR=heart rate; B) AoP=aortic pressure; C) PAP=pulmonary artery pressure; D) RAP=right atrial pressure; E) LV dP/dt=rate of change of left ventricular pressure; E) CAP=coronary artery pressure; F) CBF=coronary blood flow; and H) MVR=coronary microvascular resistance. Comparisons between groups were made using unpaired *t*-test.

Central Illustration Mechanism of Autoregulation: Proposed mechanism of intraluminal coronary pressure sensing and GPR39 stimulation and vasoconstriction (see text for details). Increased or decreased intraluminal pressure is sensed by ion channels or G-protein coupled receptors that will either increase (high pressure) or decrease (low pressure) arachidonic acid production leading to either vasoconstriction or vasodilation. 15-HETE=15-hydroxyeicosatetraenoic acid; 15-LO=15-lipooxygenase; PLA_2=phospholipase A_2. Created in https://Biorender.com

Figure 1: Breakdown of the dogs into groups and protocols. See text for details. Created in https\\Biorender.com

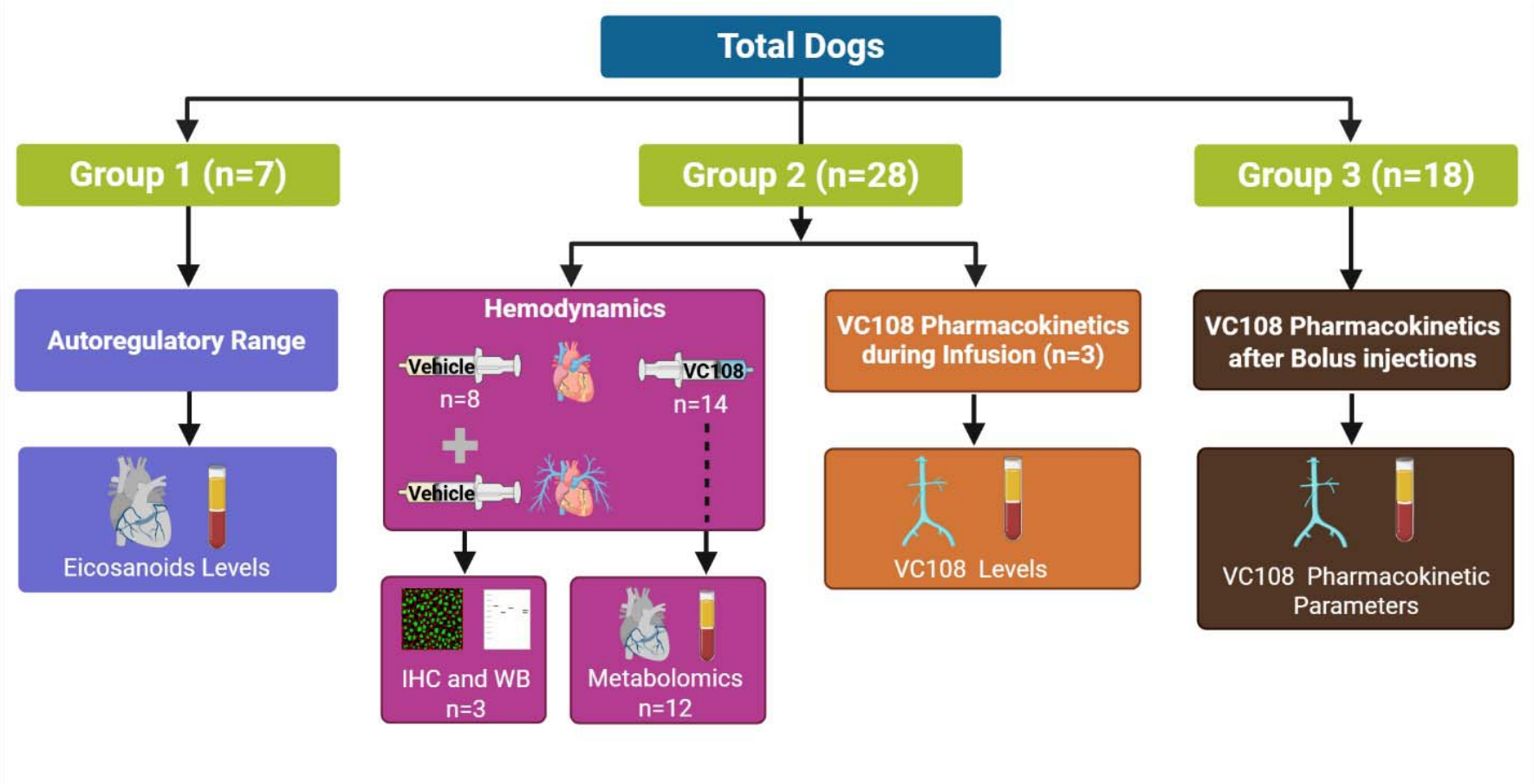

Figure 2: Examples of IHC (A) and western blot (B) of dog heart showing presence of GPR39. GPR39 (in green) is seen lining the arterioles (A). Nuclei are stained blue (DAPI). Western blot depicts a characteristic 54 kDa band for GPR39 from 3 different dogs.

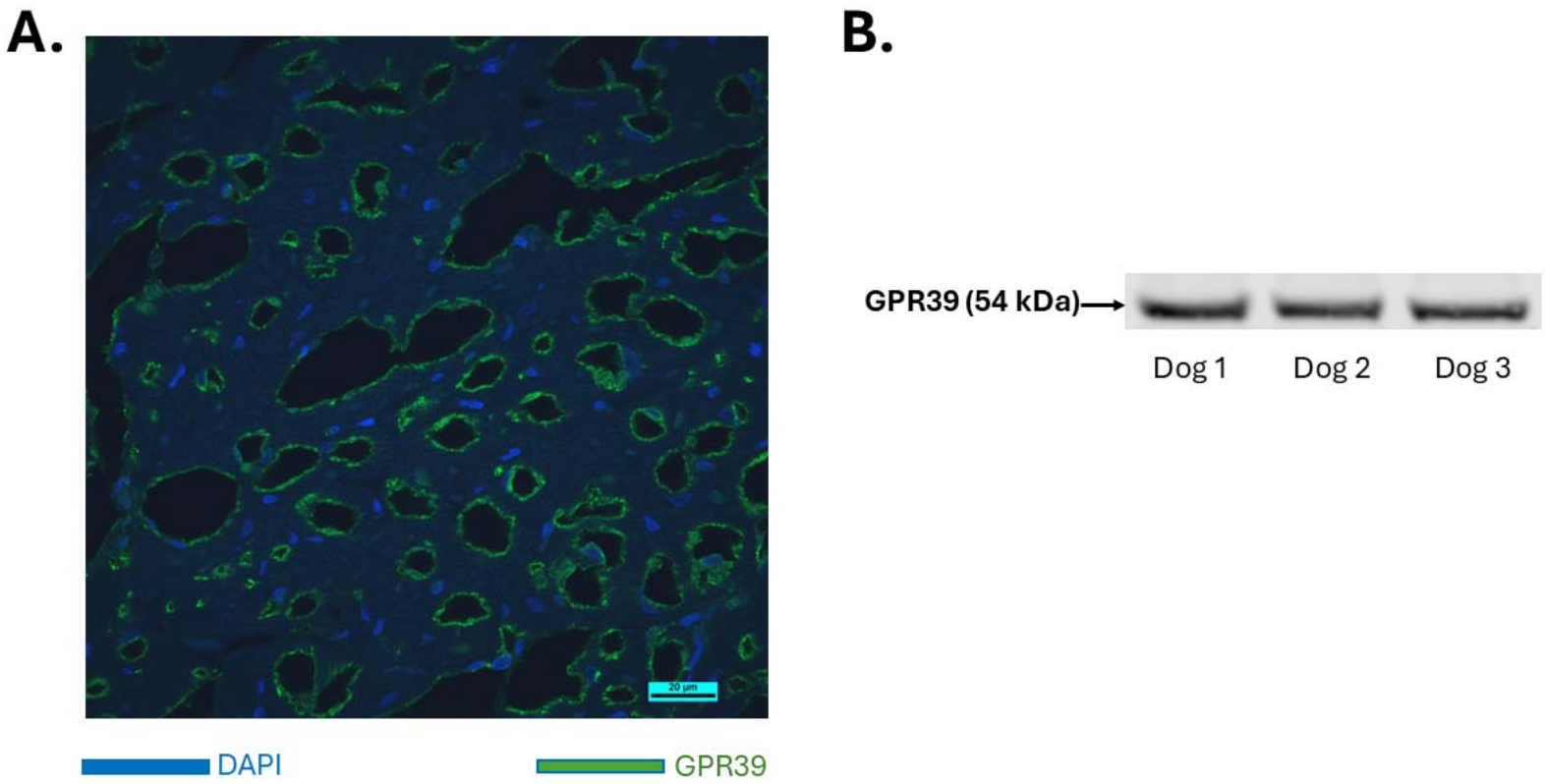

Figure 3: Relation between coronary driving pressure and anterior cardiac venous plasma levels of A)15-HETE and 14,15-EET from 7 dogs undergoing different degrees of coronary stenosis within the autoregulatory range, and B) 15-HETE/14,15-EET ratio.

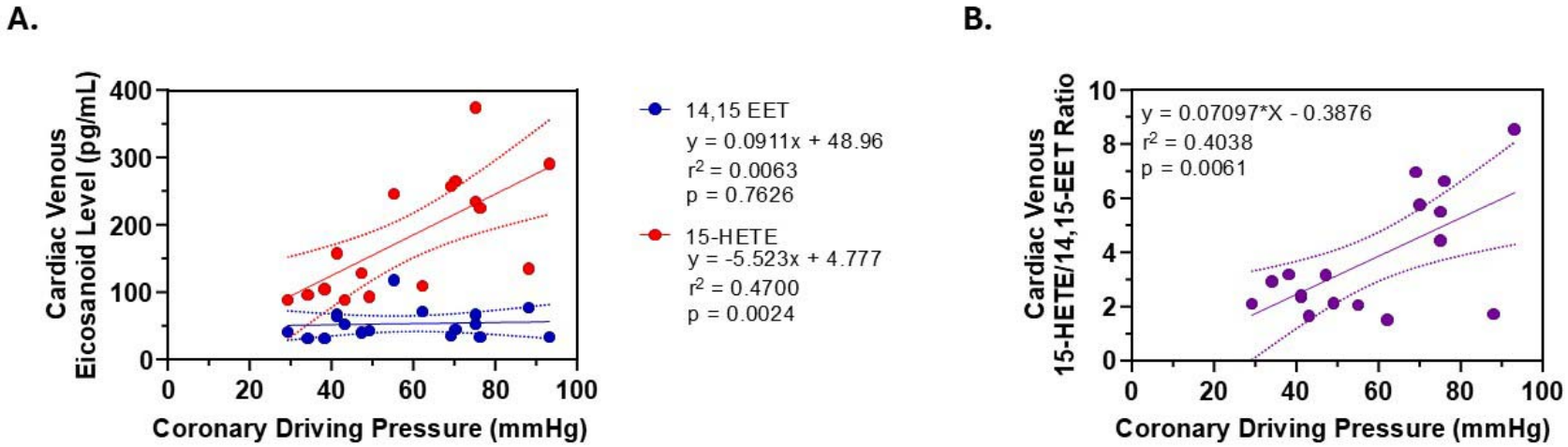

891

Figure 4: Coronary driving pressure versus coronary artery blood flow results from protocols 2 and 3. A) Data from 22 individual dogs (77 unique stages) in the absence of VC108 showing flat coronary artery blood flow over a wide range of coronary driving pressures, with decreasing flow at low coronary driving pressures. B) Aggregate results from the same animals as in panel A, showing classical coronary autoregulation over a wide range of coronary driving pressures with a decline in coronary artery flow at low coronary driving pressures. Data were fit using one phase decay least-squares analysis. C) Data from 14 of the 22 individual dogs (74 unique stages) from protocol 2 in the presence of VC108 (protocol 3) showing declining coronary artery blood flow with lowering of coronary driving pressure. D) Aggregate results from the same animals as in panel C, showing abolishment of coronary autoregulation with coronary artery blood flow becoming coronary driving pressure dependent. Data were fit using linear regression analysis.

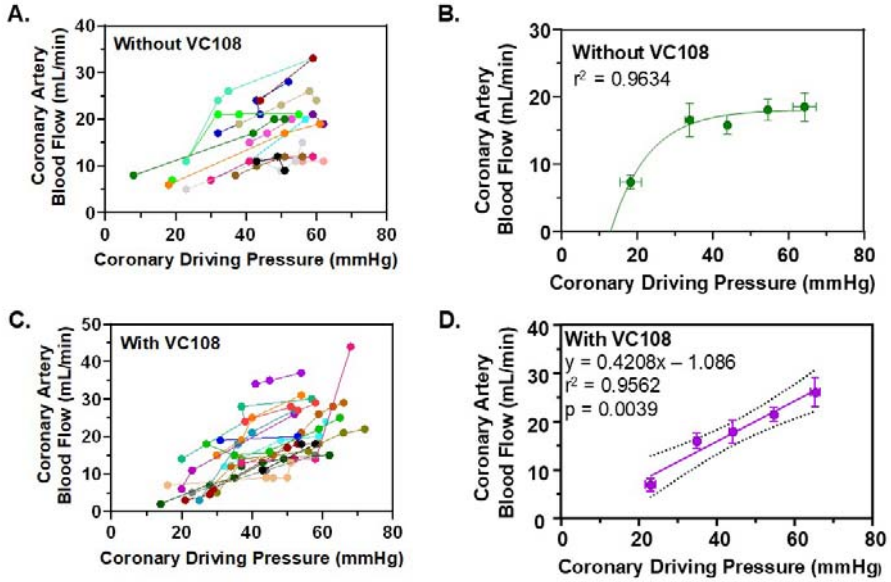
A.
Without VC108
Coronary Artery Blood Flow (mL/min)
Coronary Driving Pressure (mmHg)
B.
Without VC108
r² = 0.9634
Coronary Artery Blood Flow (mL/min)
Coronary Driving Pressure (mmHg)
C.
With VC108
Coronary Artery Blood Flow (mL/min)
Coronary Driving Pressure (mmHg)
D.
With VC108
y = 0.4208x – 1.086
r² = 0.9562
p = 0.0039
Coronary Artery Blood Flow (mL/min)
Coronary Driving Pressure (mmHg)

Figure 5: Relation between coronary driving pressure and anterior coronary vein plasma concentrations of A) adenosine and B) endothelin-1 from 12 dogs undergoing various degrees of coronary stenoses at rest.

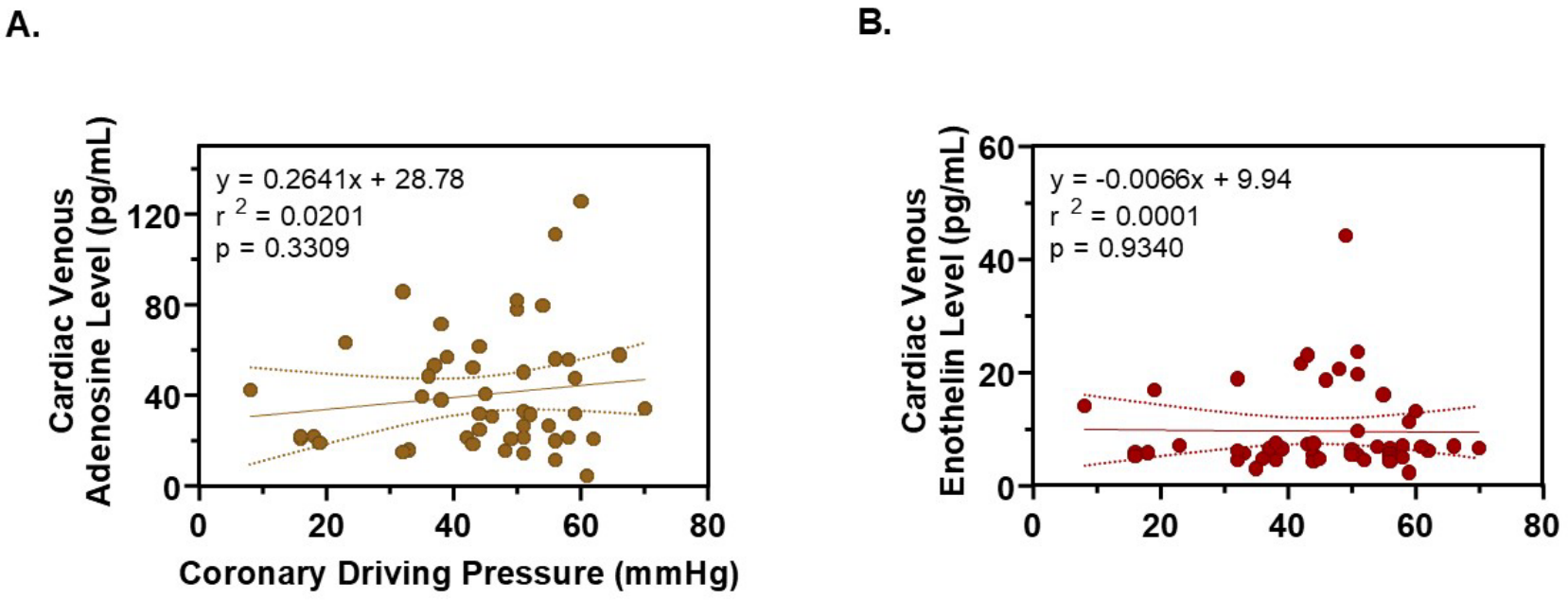

Figure 6: Relation between coronary driving pressure and anterior coronary vein plasma concentrations of A) Arachidonic acid; B) 6-keto-PGF$_{\alpha}$, (an inactive metabolite of prostaglandin I2; C) Thromboxane A2; D) Prostaglandin D2; E) Prostaglandin E2; and F) Prostaglandin F2$_{\alpha}$.

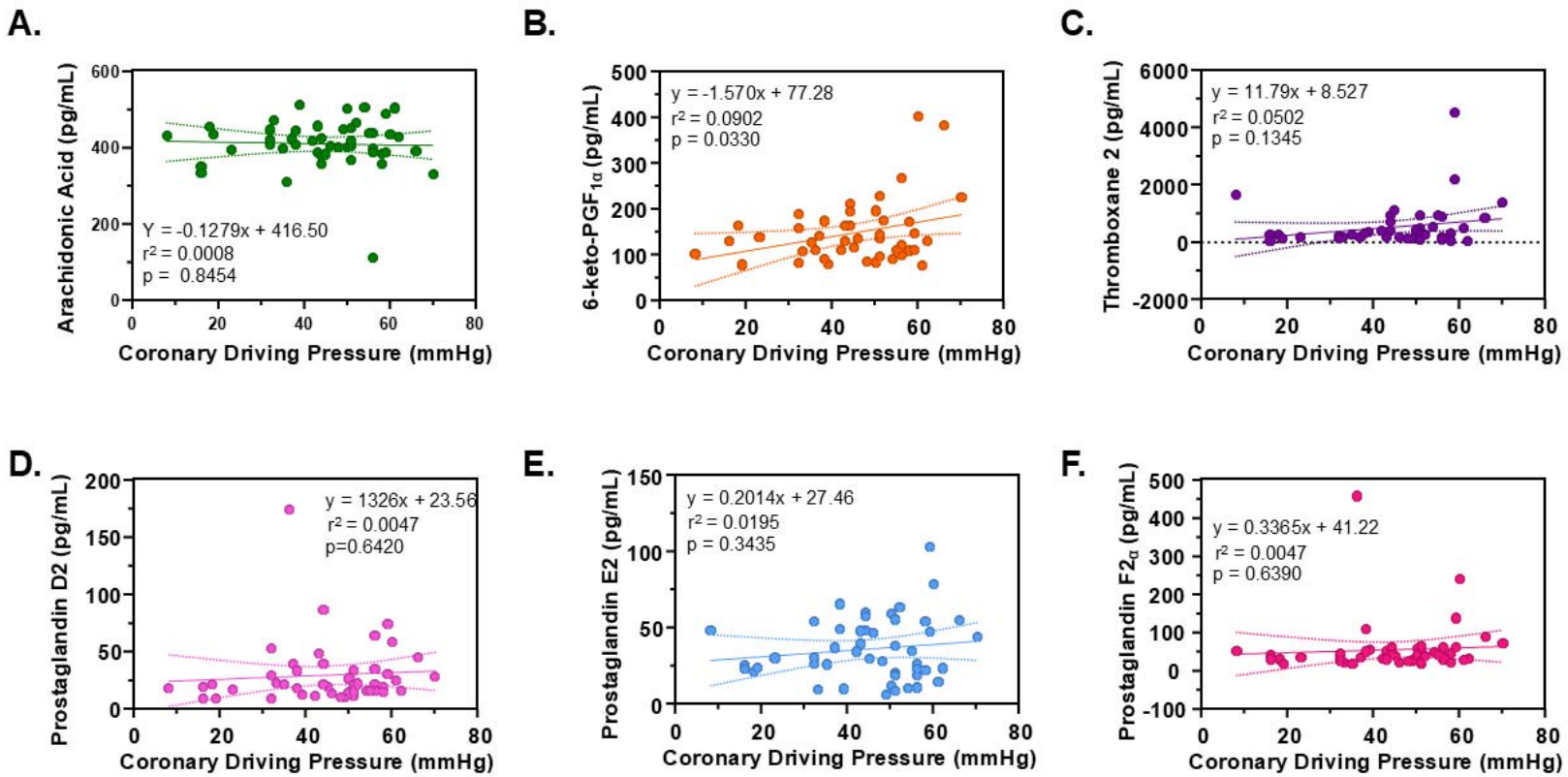

Figure 7: Percent change from baseline in systemic, pulmonary, and coronary hemodynamics with administration of Vehicle (VEH, n=11) or VC108 (n=13). A) HR=heart rate; B) AoP=aortic pressure; C) PAP=pulmonary artery pressure; D) RAP=right atrial pressure; E) LV dP/dt=rate of change of left ventricular pressure; E) CAP=coronary artery pressure; F) CBF=coronary blood flow; and H) MVR=coronary microvascular resistance. Comparisons between groups were made using unpaired *t*-test.

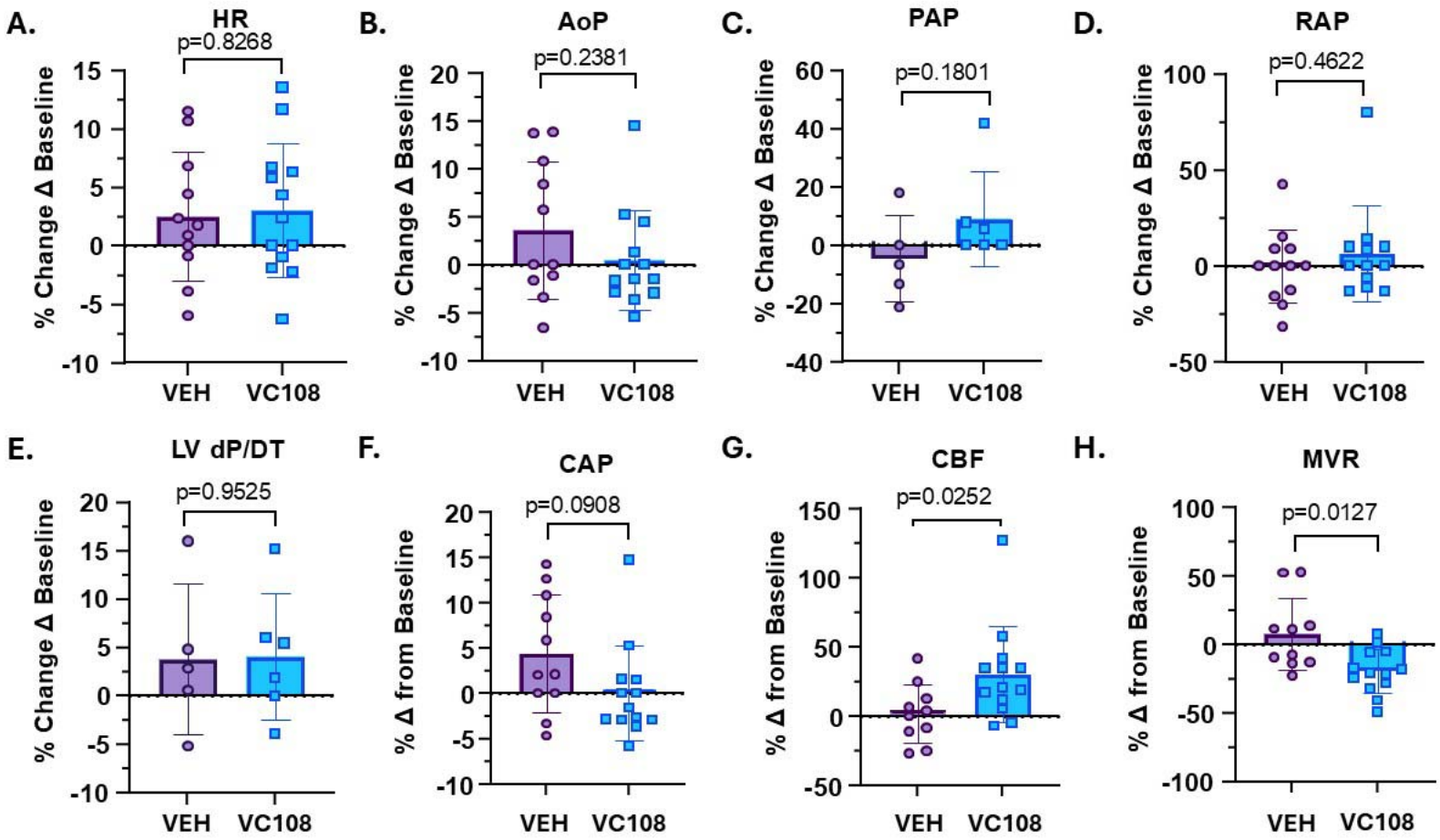
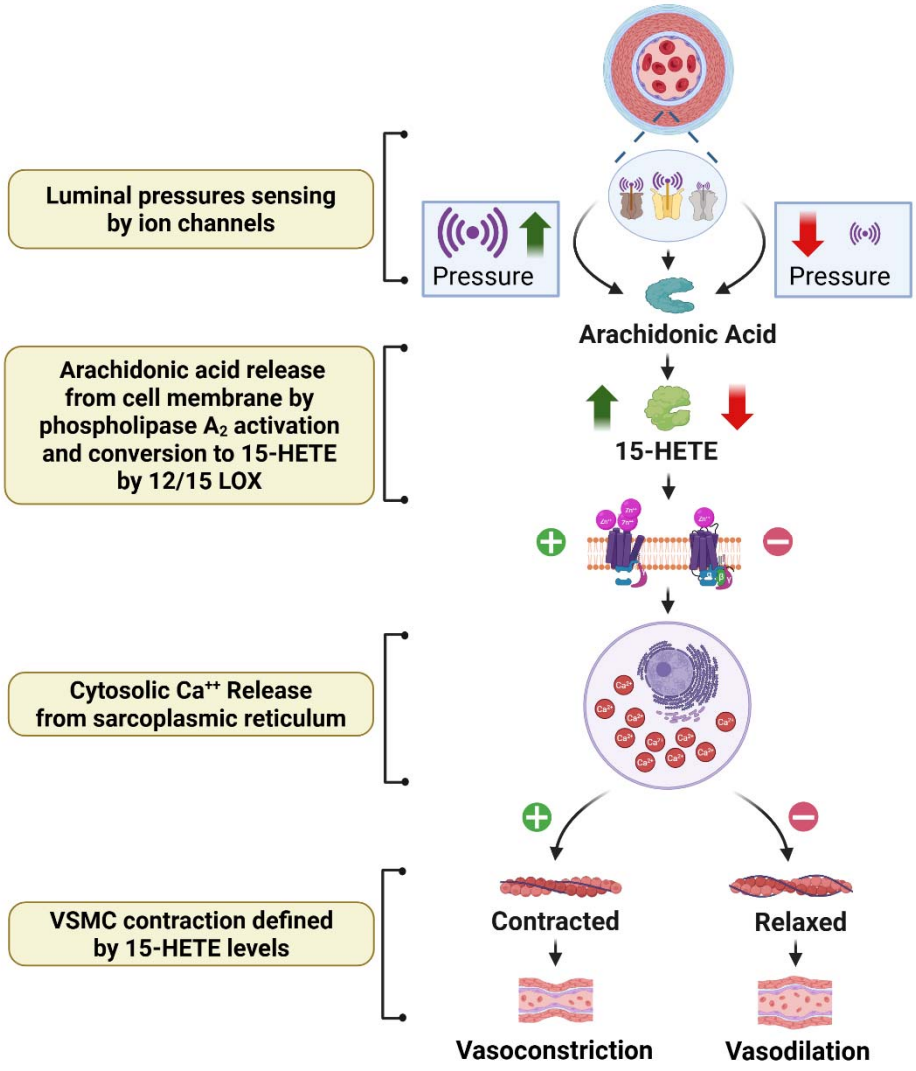
Central Illustration Mechanism of Autoregulation: Proposed mechanism of intraluminal coronary pressure sensing and GPR39 stimulation and vasoconstriction (see text for details). Increased or decreased intraluminal pressure is sensed by ion channels or G-protein coupled receptors that will either increase (high pressure) or decrease (low pressure) arachidonic acid production leading to either vasoconstriction or vasodilation. Created in https://Biorender.com